Afro-Asian Journal of Scientific Research (AAJSR)
المجلة الأفروآسيوية للبحث العلمي (AAJSR)
E-ISSN: 2959-6505
Volume 2, Issue 2, April - June 2024, Page No: 16-32
Website: https://aajsr.com/index.php/aajsr/index
SJIFactor 2023: 3.908 **0.51 :2023 (AIF) معامل التأثير العربي** **ISI 2023: 0.337**

Subspace-Based System Identification and Fault Detection for Suspension System Based on Vibration Analysis

Moamar Hamed [1*], Ali M. Aburass [2], Fengshou Gu [3]

[1] Department of Mechanical and Industrial Engineering, Faculty of Engineering, Alasmarya Islamic University, Zliten, Libya
[2] Mechanical Engineering Technology Department, Higher Institute of Science and Technology, Zawiya, Libya
[3] Centre for Efficiency & Performance Engineering, School of Computing and Engineering, University of Huddersfield, UK

*Corresponding author: m.ehmid@asmarya.edu.ly

Received: February 06, 2024	Accepted: April 02, 2023	Published: April 06, 2024

Abstract:
System identification is a technique that can be employed to obtain a mathematical representation of how a system behaves. The objectives of this research are to determine the modal parameters, such as damping coefficient and spring stiffness, and to explore an online condition monitoring system for the suspension. This will be achieved by using a MATLAB simulation of a seven degree-of-freedom (7-DOF) model of a complete vehicle. The accuracy of the simulation will be ensured by measuring only the accelerations of the vehicle's sprung mass, using subspace identification methods. Stochastic subspace identification (SSI) approaches, which just utilize output data, are employed to ascertain the whole vehicle model that remains applicable across the entire range of operation. Common issues related to suspension components include damaged or leaking shock absorbers and weakened springs. These deficiencies frequently lead to a decrease in the vehicle's overall performance. The simulation incorporates suspension flaws by introducing damage to the shock absorbers (dampers). The faults are induced by reducing the damper coefficient by 25%, 50%, and 80%. This has served as the foundation for evaluating the ride comfort, road handling, and stability of the car, as well as identifying any potential damping issues at an early stage. The cars included in this analysis of system identification exhibit non-linear dynamic behavior that is primarily influenced by the stochastic nature of road-tyre excitations. Instead of utilizing tire forces as inputs, which can be challenging to measure or predict, the inputs are based on the accelerations of the sprung masses. The vehicle's bouncing, pitching, and rolling modes are identified and described.
Stochastic Subspace Identification (SSI) algorithms provide a precise and reliable estimation of uncertain vehicle characteristics, such as the natural frequencies and damping ratio of the bounce, pitch, and roll modes for the complete vehicle model. These estimations are not affected by the initial estimates or the excitation signals used. The model results were found to closely align with the theatrical results. Furthermore, the damping estimates exhibited a significantly greater level of variability compared to the frequency estimates.
Theoretical investigation indicates that the subspace identification method, which utilizes the accelerations of sprung masses as inputs, can provide reliable estimations of model parameters such as spring stiffness and damping coefficient.

Keywords: System Identification, Vehicle Parameters, Subspace Method, Full Vehicle Model and Dynamics, Vibration Measurements.

Cite this article as: M. Hamed, A. M. Aburass, F. Gu, "Subspace-Based System Identification and Fault Detection for Suspension System Based on Vibration Analysis," *Afro-Asian Journal of Scientific Research (AAJSR),* vol. 2, no. 2, pp. 16–32, April - June 2024.

طريقة الفراغ الجزئي لتحديد معاملات واكتشاف الاعطال لنظام التعليق في السيارات باستخدام تحليل الاهتزازات

معمر إحميد[1]، على أبوراس[2]، فنغشو قو[3]
[1] قسم الهندسة الميكانيكية والصناعية، كلية الهندسة، الجامعة الأسمرية الإسلامية، زليتن، ليبيا
[2] قسم تقنية الهندسة الميكانيكية، المعهد العالي للعلوم والتقنية، الزاوية، ليبيا
[3] مركز هندسة الكفاءة والأداء، كلية الحاسبات والهندسة، جامعة هيدرسفيلد، المملكة المتحدة

الملخص

تعريف النظام هو أسلوب يمكن استخدامه للحصول على تمثيل رياضي لكيفية تصرف النظام. أهداف هذا البحث هي تحديد المعلمات النموذجية، مثل معامل التخميد وجساءة النوابض، واستكشاف نظام مراقبة حالة التعليق أونلاين. سيتم تحقيق ذلك باستخدام محاكاة ببرنامج MATLAB لنموذج سباعي درجات من الحرية (7-DOF) لمركبة كاملة. سيتم ضمان دقة المحاكاة من خلال قياس تسارع كتلة المركبة المعلقة، باستخدام طرق تحديد الفضاء الجزئي. يتم استخدام أساليب تحديد الفضاء الجزئي العشوائي(SSI) ، والتي تستخدم بيانات المخرجات فقط، للتأكد من طراز السيارة بأكمله الذي يظل قابلاً للتطبيق عبر نطاق التشغيل بأكمله.

تشمل المشكلات الشائعة المتعلقة بمكونات التعليق ممتصات الصدمات التالفة أو المتسربة والينابيع الضعيفة. تؤدي أوجه القصور هذه في كثير من الأحيان إلى انخفاض الأداء العام للمركبة. تتضمن المحاكاة عيوبًا في نظام التعليق من خلال إحداث تلف في ممتصات الصدمات (المخمدات). تحدث الأخطاء عن طريق تقليل معامل ماص الصدمات أو المخمد بنسبة 25% و50% و80%. وقد كان هذا بمثابة الأساس لتقييم راحة الركوب، والتعامل مع الطريق، واستقرار السيارة، بالإضافة إلى تحديد أي مشكلات محتملة في التخميد في مرحلة مبكرة.

تُظهر السيارات المدرجة في هذا التحليل لتحديد هوية النظام سلوكًا ديناميكيًا غير خطي يتأثر بشكل أساسي بالطبيعة العشوائية لانحراف إطارات الطريق. بدلاً من استخدام قوى الإطارات كمدخلات، والتي قد يكون من الصعب قياسها أو التنبؤ بها، تعتمد المدخلات على تسارع كتل النوابض. يتم تحديد ووصف أوضاع الارتداد والتأرجح والتدحرج للمركبة.

توفر خوارزميات تحديد الفضاء الفرعي العشوائي (SSI) تقديرًا دقيقًا وموثوقًا لخصائص السيارة غير المؤكدة، مثل الترددات الطبيعية ونسبة التخميد لأوضاع الارتداد والميل والتدحرج لنموذج السيارة الكامل. ولا تتأثر هذه التقديرات بالإشارات المستخدمة. تم العثور على نتائج النموذج تتوافق بشكل وثيق مع النتائج النظرية. علاوة على ذلك، أظهرت تقديرات التخميد مستوى أكبر بكثير من التباين مقارنة بتقديرات التردد.

يشير البحث النظري إلى أن طريقة تحديد الفضاء الجزئي، والتي تستخدم تسارع الكتل المعلقة كمدخلات، يمكن أن توفر تقديرات موثوقة لمعلمات النموذج مثل ثابت النابض ومعامل التخميد.

الكلمات المفتاحية: تعريف النظام، معلمات المركبة، طريقة الفضاء الجزئي، نموذج المركبة الكامل وديناميكياتها، قياسات الاهتزاز.

Introduction:

Suspension system performances:

Automobile designers have a difficult problem when creating suspension systems since they must consider many control factors, intricate objectives, and unpredictable disruptions. Ensuring a consistently high level of ride comfort and vehicle handling across various driving situations poses a challenging task for automobiles. From October 2010 to September 2011, the Ministry of Transport (M.O.T) gathered data [1] in the United Kingdom regarding MOT tests for almost 24.2 million automobiles. Figure 1 depicts a pie chart illustrating the proportion of failures, categorized by automobile model. The pie chart demonstrates that lighting and signalling issues constituted the largest proportion of re-tests, amounting to 19.79%. This was followed by suspension faults, which accounted for 13.18% of re-tests. The fourth most prevalent fault, at 8.75%, was related to tyre issues.

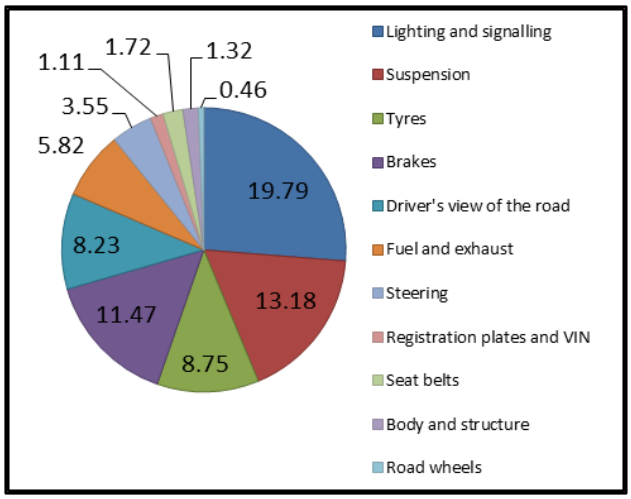

Figure 1 Percentage of failure by category for different cars.

Timely identification of irregular occurrences in automotive suspension systems helps minimize the harm inflicted on the vehicle during driving scenarios, while also enhancing passenger comfort and safety. Faults in the suspension system frequently diminish the performance of a vehicle. The user's text is "[2]." The typical issues related to suspension components include impaired or leaking shock absorbers, weakened springs, erosion of the pivot and bushing, and damage to the main support member assembly, as depicted in Figure 2 (a).

Faults in the damping system may arise from various sources, including worn seals, decreased oil flow caused by leaks, damaged mounts, and extruded or worn bushings. Each of the issues stated above can contribute to a deterioration in the performance of the shock absorber, which in turn leads to increased braking distances. As a result, the tires gradually deteriorate, leading to decreased vehicle maneuverability when turning. The user's text is "[3].".

To analyze the suspension's performance in terms of ride quality, handling, and stability of the vehicle, certain crucial parameters need to be taken into account. The parameters to be considered are wheel deflection, suspension travel, and vehicle body acceleration. The goal is to minimize the amplitude value for each of these parameters. The user's text is "[2]." Road handling is determined by the difference in position between the suspension and the road input, which is represented by (Zu - Zr). Wheel deflection is depicted in Figure 2b. Suspension travel refers to the relative displacement between the body of the vehicle and the wheel, denoted as (Zs – Zu) and illustrated in Figure 2 (b). This can be utilized to evaluate the spatial dimensions necessary to accommodate the suspension spring. The comfort of the ride is determined by the passenger's perception of the movement of the vehicle's body. This necessitates minimizing the acceleration of the vehicle body (sprung mass). ISO: 2631-1-1997[4] specifies that the acceptable range for road handling should be approximately 0.0508 m, while the minimal value for suspension travel should be approximately 0.127 m. If the root mean square (RMS) acceleration is less than 0.315 m/s^2, it is believed that the passenger will experience a high level of comfort.

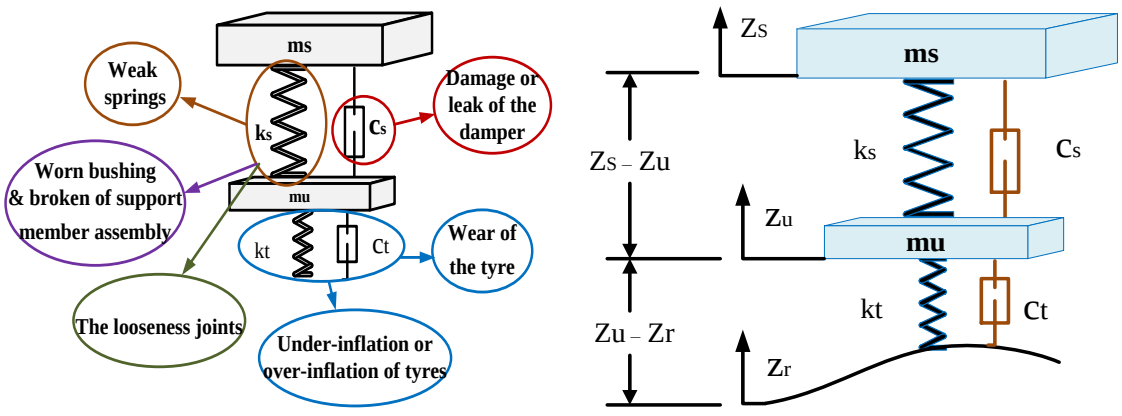

Figure 1 a: common faults in suspension systems, and b: Sketch of quarter car model.

Many researchers have examined suspension performance through the use of modeling, simulation, and experimental inquiry. Faheem [5] examined a mathematical model for a quarter automobile with two degrees of freedom (2-DOF) and a half car with four degrees of freedom (4-DOF). Rao [6] constructed a mathematical representation of a 3-degree-of-freedom (DOF) quarter automobile equipped with a semi-active suspension system. This model was employed to conduct tests on skyhook and other tactics related to semi-active suspension systems. Esslaminasa et al [7] designed a semi-active twin-tube shock absorber by creating models for one and two degrees of freedom (DOF) in a quarter vehicle design. Darus [8] utilized a state space methodology to construct a mathematical model for both a quarter automobile and a full car, employing MATLAB programs. Metallidis [9] utilized a statistical system identification technique to accurately determine the parameters and detect faults in nonlinear automobile suspension systems. Kashi [10] implemented a model-based approach for detecting defects in a vehicle control system. This approach relied on mathematical representations of the system, resulting in effective fault detection and identification of flaws that impact the system. A mathematical model for passive and active quarter car suspension systems was presented by Agharkakli et al [11]. Ikenaga et al [12] conducted a research study aimed at enhancing the road handling and riding comfort. A whole vehicle model was utilized to develop an active suspension control system that incorporates the suspension system's performance. Lu et al [13] examined the impact of vehicle speed on shock and vibration levels. They found that the influence of truck speed on the root mean square acceleration of the vibrations was significant at lower speeds but diminished at higher speeds.

Holdman [14] conducted an empirical investigation on a 3.5-ton vehicle with the aim of enhancing its handling and comfort. Three distinct damping rates were employed: a soft rate, which was two-thirds of the standard rate, the standard rate itself, and a harsh rate, which was one and a half times the standard rate. According to the results, in the passive system, it is necessary to have large damping rates for frequencies below 4Hz in order to achieve both comfort and safety. The optimal combination of comfort and safety was observed in the frequency range of 4Hz - 8Hz when a low damping rate was used.

Weispfenning [3] using a test equipment and a moving vehicle to identify malfunctions in shock absorbers and sensors. This study asserted that defects in shock absorbers led to a 20% increase in the braking distance. Lozoya-Santos [15] introduced a fault detection system to monitor the condition of an MR damper. The system is designed to monitor the transmissibility of the semi-active suspension in a quarter vehicle model. The findings of this investigation suggest that transmissibility is a reliable predictor of defective MR dampers. Tudon-Martinez [16] introduced a fault tolerant approach for identifying and isolating the defective damper. After analyzing the results, it was asserted that the presence of an oil leakage in a damper led to a 60% improvement in comfort for the regulated suspension system and an 82% improvement for the uncontrolled suspension system. Breytenbach [17] examined the debate between ride comfort and handling in relation to off-road vehicles. This study examined a novel method of a semi-active suspension system known as "4 State Semi-active Suspensions," which enables the transition between low and high damping.

Suspension System Model and Dynamics:

Development of the vehicle model operates under the assumptions that the vehicle is a rigid body, represented as sprung mass (ms), and the suspension axles are represented as unsprung mass (mu) as shown in figure 3. The suspension between the vehicle body and wheels are modelled by linear spring and damper elements and each tyre is modelled by a single linear spring and damper. The origin of coordinates is fixed in the centre of gravity (CG) of sprung mass. Using Ford Granada as a model, which adopted from Ref [18], with some emended have been added to the model for more improvement such as including the damping of the tyre, the vehicle parameters can be seen in Table 1. The equations of all motions are derived separately resulting in the equations of the body motions.

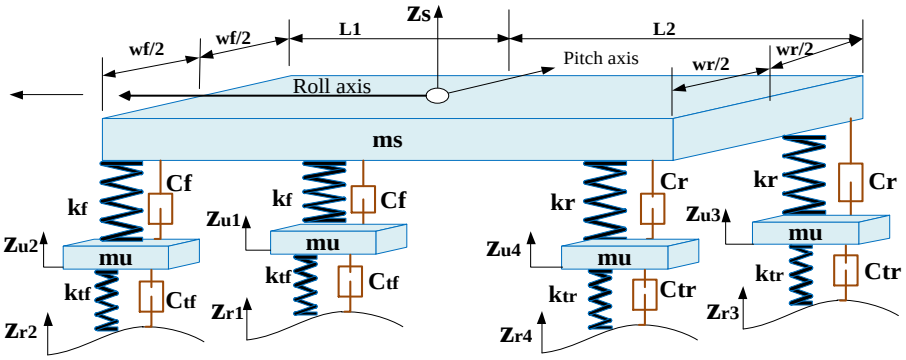

Figure 3 Full vehicle models.

Equation of motion for bouncing of sprung mass:

$$m_s\ddot{z_s} = k_f(z_{u1} - z_{s1}) + k_f(z_{u2} - z_{s2}) + k_r(z_{u3} - z_{s3}) + k_r(z_{u4} - z_{s4}) + c_f(\dot{z}_{u1} - \dot{z}_{s1}) + c_f(\dot{z}_{u2} - \dot{z}_{s2}) + c_r(\dot{z}_{u3} - \dot{z}_{s3}) + c_r(\dot{z}_{u4} - \dot{z}_{s4}) \quad (1)$$

For pitching moment of inertia of sprung mass

$$I_p\ddot{\theta} = k_f l_1(z_{u1} - z_{s1}) + k_f l_1(z_{u2} - z_{s2}) - k_r l_2(z_{u3} - z_{s3}) - k_r l_2(z_{u4} - z_{s4}) + c_f l_1(\dot{z}_{u1} - \dot{z}_{s1}) + c_f l_1(\dot{z}_{u2} - \dot{z}_{s2}) - c_r l_2(\dot{z}_{u3} - \dot{z}_{s3}) - c_r l_2(\dot{z}_{u4} - \dot{z}_{s4}) \quad (2)$$

For rolling motion of the sprung mass

$$I_r\ddot{\varphi} = \frac{k_f w_f}{2}(z_{u1} - z_{s1}) - \frac{k_f w_f}{2}(z_{u2} - z_{s2}) + \frac{k_r w_r}{2}(z_{u3} - z_{s3}) - \frac{k_r w_r}{2}(z_{u4} - z_{s4}) + \frac{c_f w_f}{2}(\dot{z}_{u1} - \dot{z}_{s1}) - \frac{c_f w_f}{2}(\dot{z}_{u2} - \dot{z}_{s2}) + \frac{c_r w_r}{2}(\dot{z}_{u3} - \dot{z}_{s3}) - \frac{c_r w_r}{2}(\dot{z}_{u4} - \dot{z}_{s4}) \quad (3)$$

For each wheel motion in vertical direction

$$m_{uf}\ddot{z}_{u1} = -k_f(z_{u1} - z_{s1}) - c_f(\dot{z}_{u1} - \dot{z}_{s1}) + k_{tf}(z_{r1} - z_{u1}) + ctf(\dot{z}_{r1} - \dot{z}_{u1}) \quad (4)$$

$$m_{uf}\ddot{z}_{u2} = -k_f(z_{u2} - z_{s2}) - c_f(\dot{z}_{u2} - \dot{z}_{s2}) + k_{tf}(z_{r2} - z_{u2}) + ctf(\dot{z}_{r2} - \dot{z}_{u2}) \quad (5)$$

$$m_{ur}\ddot{z}_{u3} = -k_r(z_{u3} - z_{s3}) - c_r(\dot{z}_{u3} - \dot{z}_{s3}) + k_{tr}(z_{r3} - z_{u3}) + ctr(\dot{z}_{r3} - \dot{z}_{u3}) \quad (6)$$

$$m_{ur}\ddot{z}_{u4} = -k_r(z_{u4} - z_{s4}) - c_r(\dot{z}_{u4} - \dot{z}_{s4}) + k_{tr}(z_{r4} - z_{u4}) + ctr(\dot{z}_{r4} - \dot{z}_{u4}) \quad (7)$$

The vertical translations of four corners of the vehicle sprung mass (1, 2, 3 and 4 shown in Fig. 4), which are just above four unsprung masses, can be represented as follows:

$$Zs1 = Zs - L1\theta + (wf/2)\varphi \quad (8)$$
$$Zs2 = Zs - L1\theta - (wf/2)\varphi \quad (9)$$
$$Zs3 = Zs + L2\theta + (wr/2)\varphi \quad (10)$$
$$Zs4 = Zs + L2\theta - (wr/2)\varphi \quad (11)$$

The equation variables and parameters of the suspension system are defined and summarized in Table 2, which is adapted from reference [18]. Except for the damping coefficient of the tires at different pressures, which were taken from [18], all other factors were considered. Modifications were also implemented to some variables in order to adhere to the specifications of the vehicle utilized in the experiment. The system can be expressed using state space matrix representations as: $\dot{x}=A(x)+B(u)$ (the input state equation) and $y=C(x)+D(u)$ (the output state equation). To simulate the state space matrices, a MATLAB code has been developed.

The road profile was calculated and created according to vehicle speeds and the height and width of the bumps by the following equation:

$$u(p) = 1/2\ a\ * \sin(2 * \pi * Fp * t) \quad (12)$$

The road profile was also assumed to be a single bump with a sin wave shape. Where a is the bump height (50 mm), Fp is the frequency of the bump (calculated in consideration of the length of the bump and the vehicle speed) and t is the time for the vehicle crossing the bump. In this study, the bump profile is 500 mm in width and 50 mm height and for validation purposes, the models were simulated at the speed of 8 km/hr.

Experimental set up and test procedure for general validation

To validate the theoretical model, a front wheel drive Vauxhall ZAFIRA (2001) car, equipped with two different sensors was used. The sensors mounted on the car include: (1) a vibration sensor with a sensitivity of (3.770 pc/ms-2) mounted on the upper mounting point of the front left shock absorber, and (2) a dynamic tyre pressure sensor (DTPS) with a sensitivity of (11.43 Pc/0.1Mpa) connected to the valve stem of the front left wheel. The pressure sensor was situated in the centre rim of the front left wheel and the vibration sensor on the inside of the car. They were positioned in these locations subsequent to their assembly and connection to the wireless sensor nodes (transmitters). Inside the automobile, the gateway (receiver) was furnished with a laptop. In order to guarantee a reliable installation of the sensors, the University of Huddersfield developed and produced two distinct adapters. Furthermore, a wireless measurement system was devised and implemented on the vehicle to provide a comprehensive distant measurement of the extracted vibration and pressure data.

Alternatively, one can use system identification techniques to obtain a reliable approximation of the unknown parameters and linear equivalent dynamic properties of the tire-road interface, given the provided loading and operating conditions.

Subspace-based system identification for suspension system

During modal analysis of vibrating structures, it is common for the operating conditions to be significantly different from those used in laboratory tests. One significant distinction is that excitations cannot be measured under natural loading conditions and are typically non-stationary. This does not imply that laboratory results are invalid, but rather that new methodologies are required for in-operation treatment. Currently, subspace-based techniques are utilized and have been demonstrated to be effective for estimating modal parameters such as natural frequencies, damping ratios, and mode shapes.The number 19 is enclosed in square brackets.

Dong et al[18] computed the modal parameters and mass moments of inertia of an on-road vehicle by using subspace identification methods to measure the accelerations of the vehicle's sprung mass and unsprung masses. This study compares two subspace identification approaches, one utilizing input/output data and the other utilizing output data solely, specifically focusing on the highly damped modes. Theoretical examination of this research indicates that the subspace identification approach, which utilizes accelerations of unsprung masses as inputs, yields more precise findings compared to the method that uses road-tyre forces as inputs, particularly when the vehicle speed is not very high. Vehicle model parameters can be determined online by analyzing the vehicle's roll and yaw dynamics. Yang et al [19] utilized a system identification technique to ascertain the lateral dynamics of an articulated freight vehicle under three distinct steering excitations. This study utilized a pseudo-random binary sequence (PRBS) excitation signal instead of the conventional ramp step (RS) and quasi-impulse (QI) steering inputs to excite the modes. The results demonstrate that the vehicle transfer function may be precisely characterized using PRBS and QI excitations.

Russo et al [20] presented a method for estimating car parameters by utilizing the Kalman filter to analyze the vehicle's regular on-road handling maneuvers. Wenzel et al [21] conducted further research on the dual extended Kalman filter technique to determine vehicle statuses and model parameters. Arikana et al [22] presented the identification of linear handling models for road vehicles using structural identifiability analysis and tests to predict the vehicle's parameters. The study's findings demonstrate that the identified model effectively tracks the system reaction. The researchers Xi-Qiang Guan et al [23] utilized subspace identification methods to estimate the dynamic model of the vehicle's handling and predict its performance in handling. These estimators necessitate sophisticated measuring techniques or precise tyre models to assess the interactions between the tyre and the road. However, the accuracy of the analysis may be compromised by inaccuracies stemming from the tyre model's precision or the tyre's state, including wear and inflation pressures.

The process of system identification is closely linked to the specific attributes of the input signal. Various system identification investigations have utilized a diverse set of input signals, including single harmonic and impulse signals [19]. The number 24 is enclosed in square brackets. The choice of the input signal is generally determined by the qualitative behavior of the system and involves two significant factors. The primary factor to consider is the form and frequency composition of the input signals, which need to be chosen in order to effectively stimulate all significant modes. Another crucial factor to examine is the cross correlation between the input signal and the noise present in the measured signals [25]. The ideal input signal should possess a broad frequency range in order to elicit all significant dynamic modes and provide a relatively precise estimation of the system parameters. While an impulse function is often regarded as an optimal input signal since it produces a uniform power spectrum across a broad range of frequencies, a pseudo random white noise signal is commonly utilized instead due to the challenges involved in generating an ideal impulse.

This research utilizes subspace identification methods to determine the parameters (matrices) of state space models. It also explores a condition monitoring system for suspension by conducting a MATLAB simulation of a seven degree-of-freedom (7-DOF) model for a full vehicle. The accuracy of the system is achieved by measuring the accelerations of the vehicle's sprung mass, which occur randomly in nature. These measurements are analyzed using subspace identification methods.

Basic theory on subspace identification algorithms:
A discrete time state space model can be represented as follows:

$$\mathrm{X(k+1)} = Ax(k) + Bf(k) \quad \text{..... (13)}$$
$$y(k) = Cx(k) + Dx(k) \quad \text{..... (14)}$$

Equations 13 and 14 contain the matrix A which is the state transition matrix that completely characterizes the dynamics of the system by its eigenvalues; B is the input influence matrix that connects inputs; C is the output influence matrix that specifies how the internal states are transformed to the outside; and D is the direct transmission matrix. The vectors $f(k)$, $y(k)$ and $X(k)$ are the inputs, outputs and states respectively of the system at time instant k.
To consider process noise and measurement noise of the model, noise vectors $w(k)$, and $v(k)$, are added into the model:

$$\mathrm{X(k+1)} = Ax(k) + Bf(k) + w(k) \quad \text{..... (15)}$$
$$y(k) = Cx(k) + Dx(k) + v(k) \quad \text{..... (16)}$$

The state space models (15 and 16) are called the deterministic–stochastic discrete time states pace model, $w(k)$ and $v(k)$ are zero mean, white noise vector sequences with covariance matrix:

$$E\left\{\begin{pmatrix} w(p) \\ v(p) \end{pmatrix}\left(w(q)^T \quad v(q)^T \right)\right\} = \begin{pmatrix} Q & S \\ S^T & R \end{pmatrix} \delta_{pq} \geq 0 \quad \text{..... (17)}$$

In Eq. (17), E denotes the expectation operator and δ_{pq} the Kronecker delta.
If the input vector $f(k)$ cannot be measured, the state space models (15 and 16) become the following models (6 and 7), which is called the stochastic state space model:

$$\mathrm{X(k+1)} = Ax(k) + w(k) \quad \text{..... (18)}$$
$$y(k) = Cx(k) + v(k) \quad \text{..... (19)}$$

The identification problem for the state space models (13 and 14), (15 and 16) and (18 and 19) can be stated as follows: given (s) inputs $f(1), f(2), \ldots\ldots\ldots f(n)$ and outputs (m) $y(1), y(2) \ldots\ldots\ldots y(m)$
The key steps to solve the identification problem for the state space model are, first to specify the order (n) of the unknown system and the second to specify the system matrixes $Ax,\ B(k), Cx\ and\ Dx$.

Subspace identification algorithms initially perform QR decomposition (also known as QR factorization) to calculate the orthogonal or oblique projection of input and output data matrices. This is followed by singular value decomposition (SVD) to determine the order, observability matrix, and state sequence. Next, the state space model is obtained by solving a least squares problem. The term "subspace" refers to the model parameters of a linear system that are derived from either the row or column subspace of a specific matrix. This matrix is constructed using the input/output data. Subspace identification utilizes non-iterative methods from numerical linear algebra, such as QR decomposition and SVD. Therefore, there are no issues with convergence and the numerical stability is assured.

As presented by Reynders et al [26], subspace identification involves the choice of two parameters: i, which is half the number of block rows of the Hankel matrices, and j, which is the number of their columns. As $j \to \infty$ ensures strongly consistent estimates for the system matrices A, B, C and D, it is obvious that for j the largest possible value should be chosen. In practice, the quality of the identified system model depends on half the number of block rows i. A solution is to choose i as large as possible, but then calculation time and memory usage might become excessive. Therefore, for the stochastic subspace identification algorithm, the half number of block rows i in the output Henkel matrices should be chosen such that $i \geq f_s/(2f_0)$, where f_s is the sampling frequency and f_0 is the lowest frequency of interest.

To identify modal parameters, the estimated system matrix A can be decomposed by eigen-decomposition as $A = \Psi\Lambda\Psi^{-1}$, where Ψ is the Eigen vector matrix and Λ = diag(λ_{di}) is the diagonal Eigen value matrix. The matrix Λ contains the n/2 discrete time eigenvalues λ_{di} and $\lambda^*{}_{di}$ in complex conjugated pairs, which are directly related to the frequency and damping properties of the system. The discrete-time Eigen values can be converted to continuous time Eigen values λ_{ci} = λ_{di}/Δt where Δt is the time step of the digital data acquisition system. Then the undamped natural frequencies f_n and damping ratios ζ_i can be easily calculated from the conjugate pair of complex-valued eigenvalues: λ_{ci}, $\lambda^*{}_{ci} = -2\pi\,\zeta_i\,f_n \pm J(2\pi\,f_n)\sqrt{1-\zeta_i{}^2}$.

The eigenvectors Ψ have no physical interpretation because the states of an identified state-space model have no direct physical meaning. However, using the identified matrix C, the observed parts of the eigenvectors Ψ can be calculated: $\emptyset = C\Psi$

Results and discussion

Model validation using sin wave shape road–tyre excitations as inputs:

The model was verified using empirical data obtained during the operation of the vehicle at a velocity of 8km/h, traversing Bump 1 (situated within the confines of The University of Huddersfield). The dimensions of the bump profile were 5.80 m in width, 0.50 m in length, and 0.050 m in height. These measurements were used as the input for the system. The vehicle response was analyzed using MATLAB software. Figure 5 illustrates the vehicle body's acceleration over time, as determined by model simulation and experimental data. After analyzing the experimental findings, it is evident that the model well predicts the suspension performance.

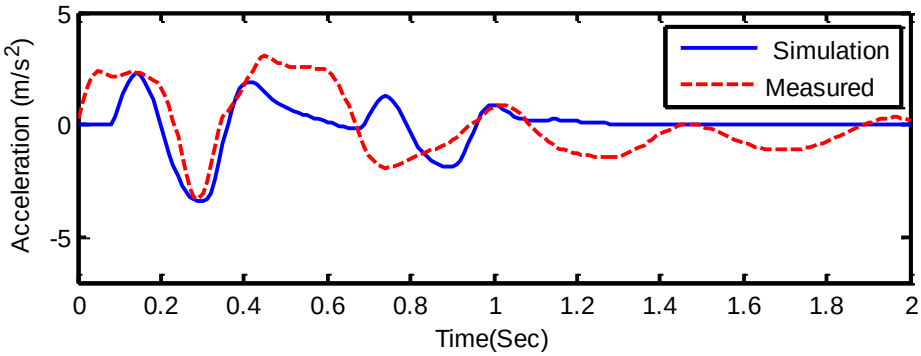

Figure 4 Vibration (acceleration) of suspension simulation and experimental.

Figure 5 (a) displays the road profile plots in the time domain for both the front and rear wheels of the vehicle. In the simulation investigation, the system assumes that road disturbance is the input. Figure 5 (b) illustrates how changing the damping coefficients affects the reaction of the vehicle body. These data indicate that higher damping coefficients lead to a decrease in the amplitude of the relative displacement of the car body.

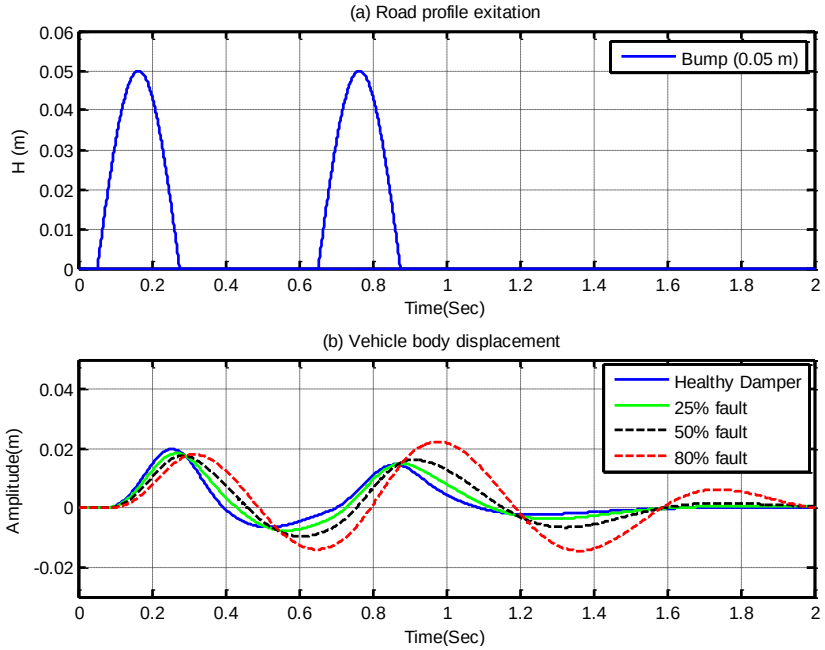

Figure 5 (a): Road profile excitation and Figure 5 (b): Displacement of vehicle body for different damping coefficients.

Figure 6 illustrates the movement of four wheels (unsprung mass) with varying damping coefficients in the time domain. The results indicate that the amplitude or peak value of the wheels reduces as the damping value decreases. This suggests that alterations to the damping coefficients can potentially impact the performance of the suspension.

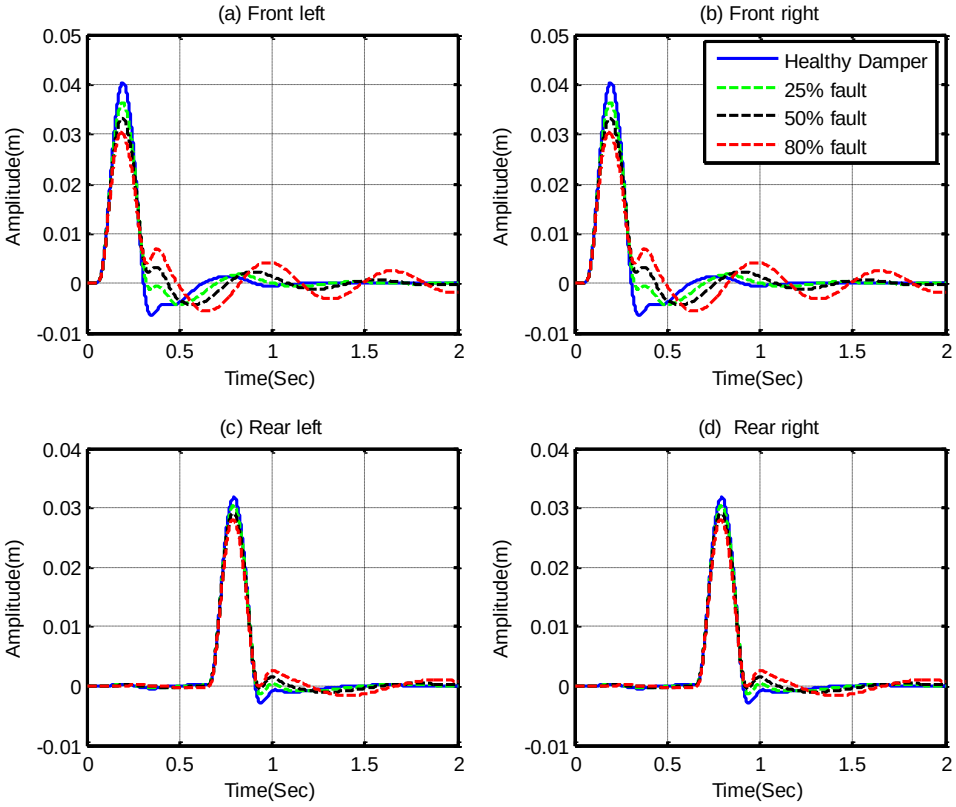

Figure 6 Vehicle wheel displacement with different damping coefficients.

An evaluation of various parameters, including wheel deflection, suspension travel, and acceleration of the vehicle body, was conducted to examine the impact of suspension damping level on suspension performance. This analysis encompasses factors such as ride quality, handling, and vehicle stability.

The road handling profile, specifically the wheel deflection, of a vehicle is determined by the contact forces between the road surface and the vehicle tire, denoted as zu and zr. In this simulation, the wheel deflections were measured to be around 0.015 m, 0.0154 m, 0.148 m, and 0.0133 m for a healthy damper, a damper with 25% fault, a damper with 50% fault, and a damper with 80% fault, respectively. These measurements are shown in Figure 7 (a). No significant alterations in the maximum magnitude of the wheel deflection can be discerned from this diagram. Nevertheless, it is worth mentioning that the vertical deflection does not diminish rapidly when faulty dampers are present, especially those with 80% and 50% defects. When compared to the specified road handling standards outlined in ISO: 2631-1-1997 [4], which need a range of 0.0508 m, this range is deemed adequate. The suspension travel refers to the relative displacement between the vehicle body and the wheel, denoted as (zs – zu) in Figure 7 (b). From this figure, it is evident that increasing the damping coefficient results in a decrease in suspension travel. Therefore, in order to minimize suspension travel, a greater damping ratio is necessary. According to ISO: 2631-1-1997 [4], a passenger is considered to experience a high level of comfort if the root mean square (RMS) acceleration is less than 0.315 m/s^2.

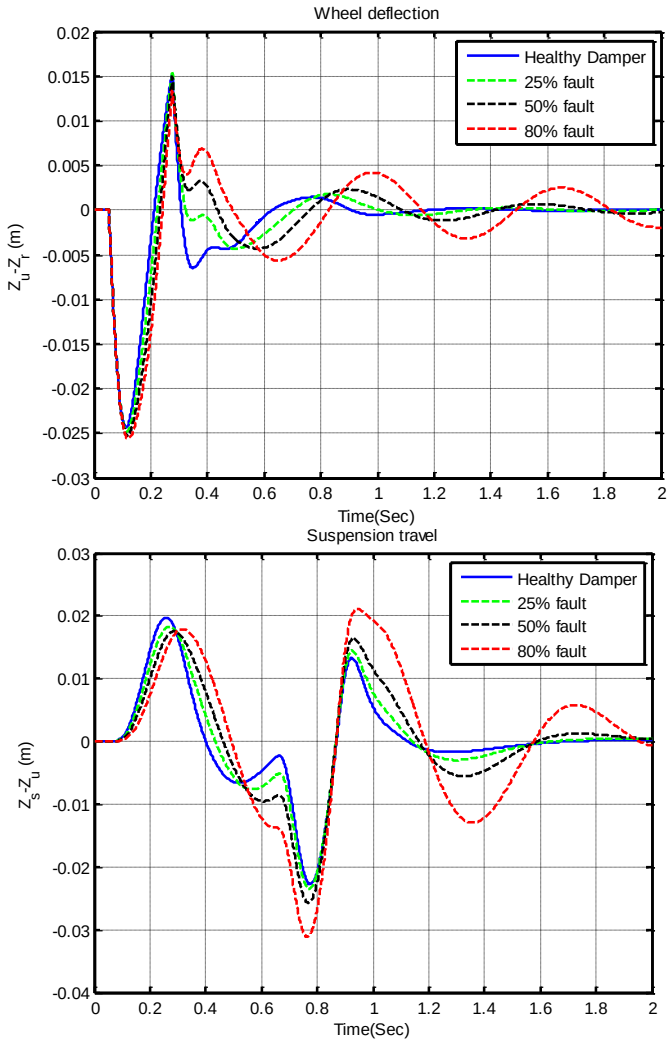

Figure 7 (a) Wheel deflections for different damping coefficients and figure 7 (b) suspension travels for different damping coefficients.

In Figure 8 (a), the magnitudes of the vertical acceleration were amplified within the range of the vehicle body (sprung mass) as the damping of the shock absorber was heightened. Increasing the shock absorber damping resulted in improved comfort for the passenger when the excitation frequencies closely matched the resonance frequency of the vehicle body. Nevertheless, the vertical acceleration does not diminish rapidly as the damping decreases.

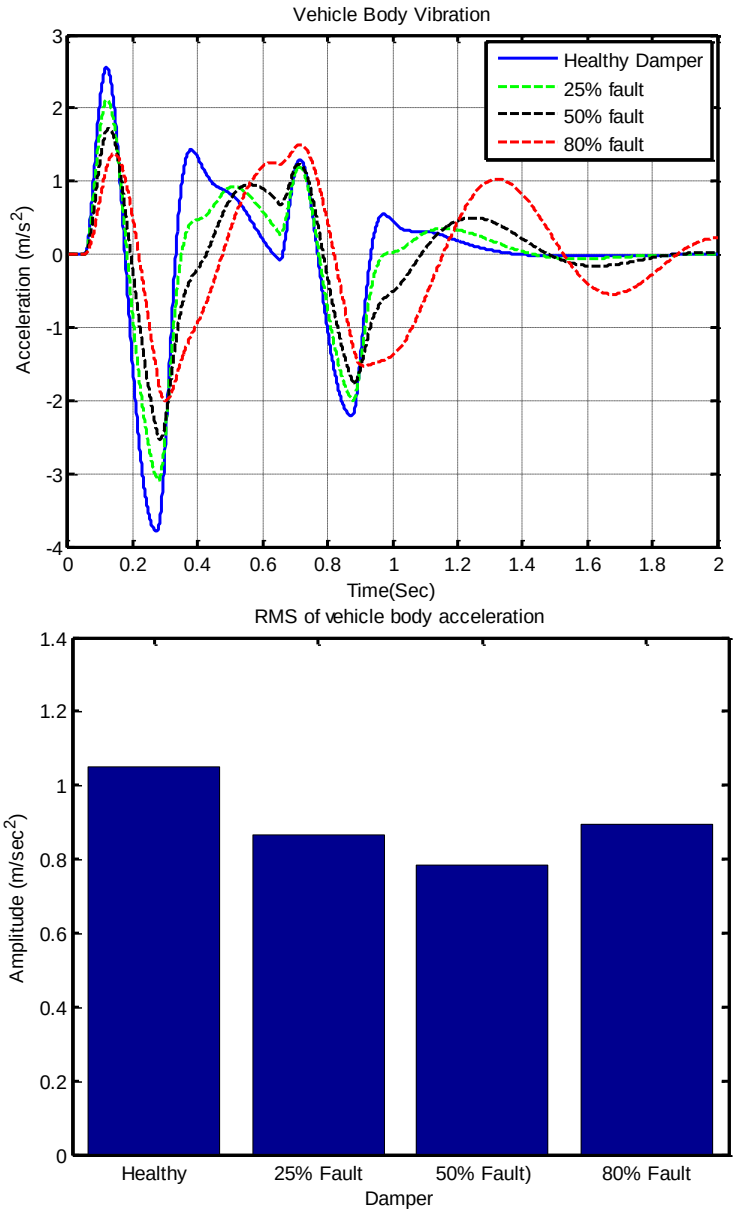

Figure 8 (a) Acceleration of the vehicle body for different damping coefficients and Figure 8 (b) RMS for acceleration of the vehicle body for different damping coefficients.

Figure 8 (b) illustrates a standard representation of the root mean square (RMS) value for the acceleration of the vehicle body. The graph displays several damping values, including healthy damping, 25% damping, 50% damping, and 80% damping fault. The results indicate that reducing the damping coefficient leads to a decrease in the acceleration of the vehicle body in the scenarios of 25% and 50% faults. Nevertheless, there is a little rise in the vehicle body's acceleration in relation to the damping, despite an 80% defect.

Subspace identification results for the seven DOF vehicle model:

The subspace identification approaches are categorized as deterministic, stochastic, and combination deterministic-stochastic algorithms based on the extent to which system inputs may be measured or partly measured [16]. Due to the assumption of unmeasured input white noise, the stochastic system identification problem can be seen as an output-only system identification method. This makes it well-suited for operational modal analysis [17–20] and vibration-based structural health monitoring [21,22] applications where input forces are not available. Hence, the stochastic subspace identification technique is employed solely with the output data to determine the undamped natural frequencies and damping ratios of the bounce, pitch, and roll modes.

Using vehicle parameters provided in Table1 in Appendix, the undamped natural frequencies f_n and damping ratios ζ_i for the 7-dof vehicle model are shown in Table1, where the first three modes are bounce, pitch and roll mode, respectively.

Table 1 undamped natural frequencies f_n and damping ratios ζ_i for the 7-dof vehicle model.

Mode	1(bounce)	2(pitch)	3(roll)	4(fl-w)	5(fr-w)	6(rl-w)	7(rr-w)
$f_n\ (Hz)$	1.037	1.288	1.604	10.9346	10.9358	11.4374	11.4374
ζ_i	0.0263	0.0247	0.0351	0.0247	0.0247	0.0262	0.0262

Two cases are included to study the effects of road–tyre excitations. The first case is that road–tyre excitations are simulated as white Gaussian random processes and vehicle speed is zero; in the second case, same excitations are used as the first case, but vehicle speed was considered by calculating the effect of wheel base filtering. When a vehicle is running, one important effect called wheel base filtering should be considered. Wheelbase filtering causes an effect that, the excitations applied to the front and rear wheels are not independent, and the rear wheels are excited by the same forcing function as the front ones with a delay $T = (l1 + l2)/v$, the time needed to travel a distance equal to the wheelbase [11]. Clearly, wheelbase filtering introduces a dependence of the response of the system on the speed.

Figure 9 (a) displays the frequency response function of the vertical bounce, pitch, and roll responses of the body and the four wheels (front-left, front-right, rear-left, and rear-right) correspondingly. The frequencies of vehicle bounce, pitch, and roll are typically within the range of 1 to 3 Hz, whereas the frequencies of the wheels are approximately 10 to 13 Hz. The frequency response of the bounce, pitch, and roll modes is depicted in Figure 9 (b). It is evident that the bounce and pitch frequencies fall within a similar range and have nearly identical amplitudes. However, the roll frequency spans a wider range compared to the bounce and pitch frequencies and also exhibits the highest amplitude. This suggests that the roll frequency has a greater impact on the simulation.

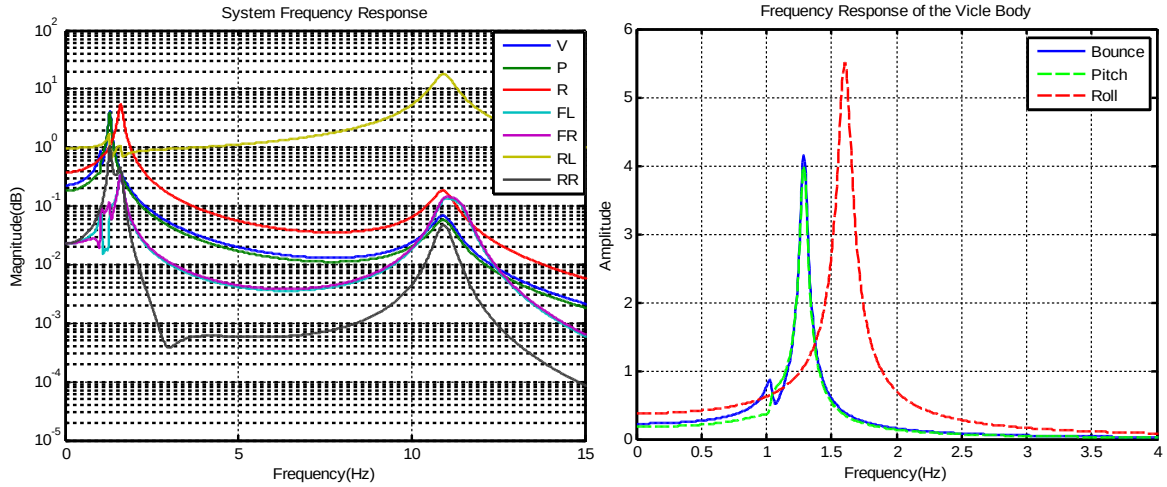

Figure 9 (a) frequency response function of the body and the four wheels (front-left, front-right, rear-left and rear-right), and figure 9 (b) Frequency response of the bounce, pitch and roll modes.

Subspace identification methods may automatically detect and isolate bounce, pitch, and roll modes of a vehicle by utilizing random excitation forces as inputs. Additionally, these methods are able to eliminate computational modes. The figure 10 (a) displays the raw data acquired from the simulation, showcasing the displacement, velocity, and acceleration of the bounce, pitch, and roll of both the vehicle body and the four wheels. Analyze the frequency responses (normalized) of the vertical displacement of sprung masses at four corners (1, 2, 3, and 4) as shown in Figure 4. This analysis is conducted when the cars are subjected to four road-tyre excitations, which are simulated as white Gaussian random processes.

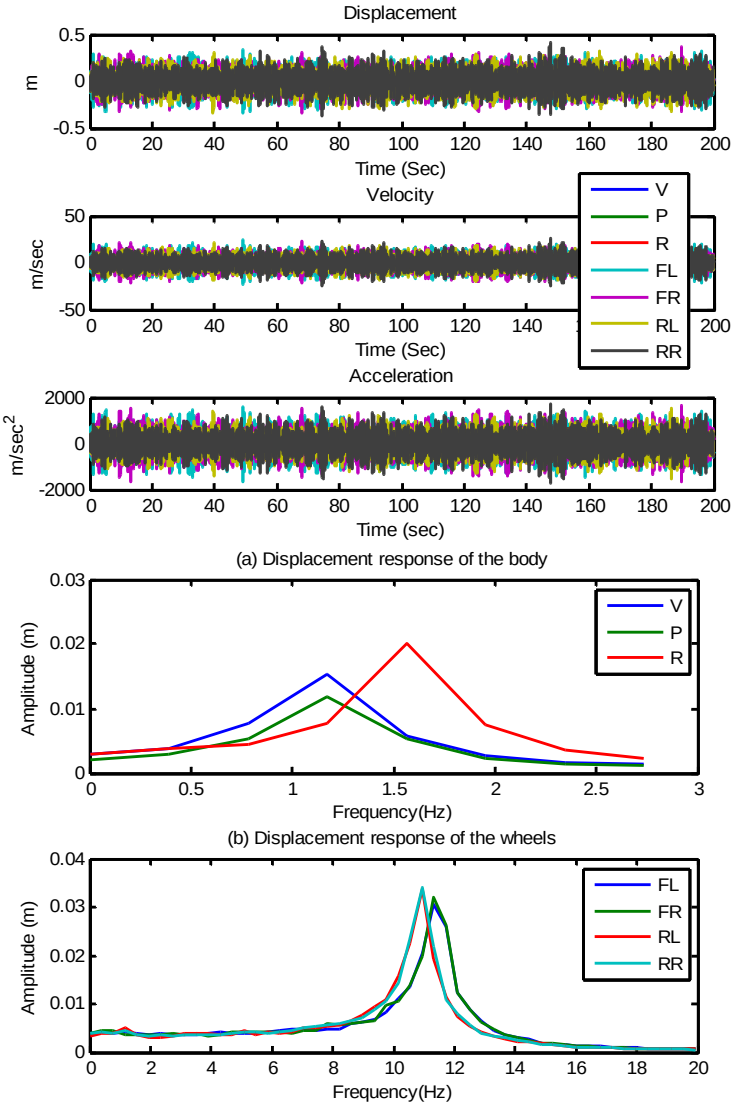

Figure 10 (a) The raw data of displacement, velocity and acceleration of the whole model, and figure 10 (b) displacement response of the body in the top and the displacement of the wheels in the bottom.

For more focus on the vehicle body responses, figure 10 (b) in the top, illustrates the displacement response of the bounce, pitch and roll of the vehicle body, and also it can be noted that, the roll frequency has the biggest amplitude and more influence on the vehicle responses. Figure 10 (b) in the bottom presents the displacements of the four wheels, which almost lie in the range of 10 – 13 Hz. To use the accelerations of the vehicle body as inputs for the model, accelerations of the vehicle body were transited from their centre of gravity to each corner of the vehicle; these translations were calculated by using equations (8, 9, 10 and 11). Figure 11 (a) shows the displacement response of the body at the four corners, and also presents the power spectrum density (PDS) at each corner, which will be used as inputs of the model to estimate the natural frequency and damping ratio for each mode. Figure 11 (b) shows the spectrum of the body at the four corners, and also presents the spectrum of correlation of each sensor with the use of sensor number one as a reference, in order to ensure the correct correlations between all sensors at each corner.

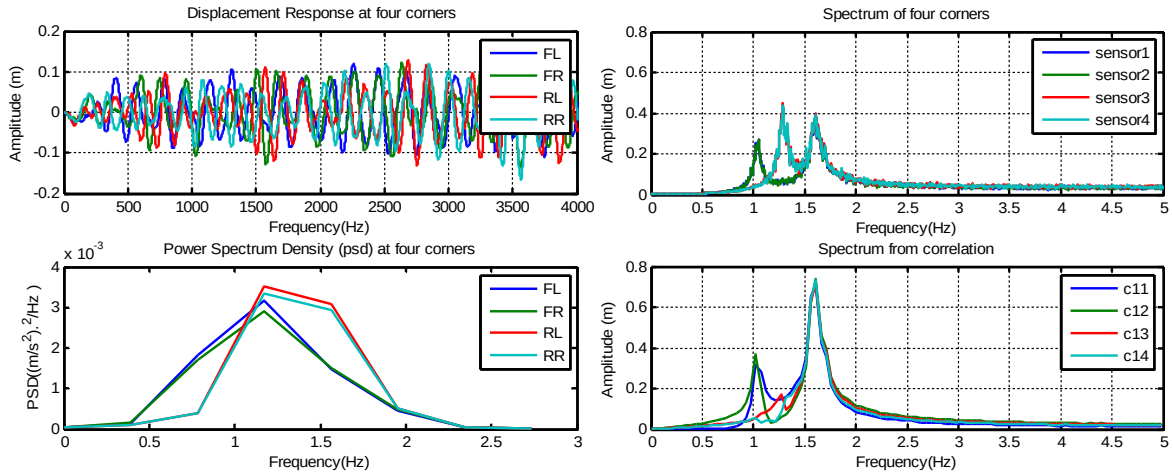

Figure 11 (a) displacement response and PDS of the body at the four corners, and Figure 11 (b) shows the spectrum of the body at the four corners and spectrum from correlations.

Figure 12 illustrates the stabilization diagram for the system, where, frequencies and damping estimated from multi-order system identification are plotted against the model order. From the modes common to many models and using further stabilization criteria, such as a threshold on damping values, low variation between modes and mode shapes of successive orders etc., the final estimated model is obtained. It can be noted from this figure that, in the region of the low frequency the frequency estimation, damping ratio and modal shape show some fluctuations, and finally the modes come to more stability to obtain more accurate frequency modes.

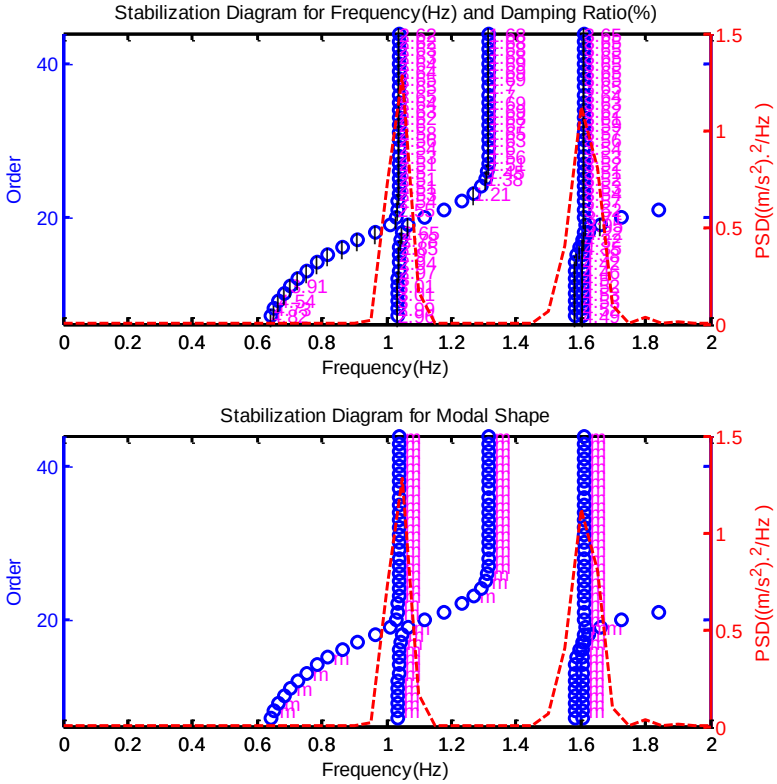

Figure 12 The stabilization diagram for the system.

Stochastic subspace identification is utilized to determine the undamped natural frequencies and damping ratios of the bounce, pitch, and roll modes only based on output data. In the initial scenario of the simulation, road-tyre excitations are modeled as white Gaussian random processes, while the vehicle speed is set to zero. Figure 13 displays the results of subspace identification, comparing the theoretical values (calculated from equations) represented by light blue bars, with the values obtained

from the model, represented by pink bars. The comparison is made for the undamped natural frequencies and damping ratios of the bounce, pitch, and roll modes, respectively. It is evident from this figure that the calculation of damping ratio exhibits greater variability compared to the natural frequencies. In this simulation, a sampling frequency of 100 Hz is chosen. As a result, the number of block rows, denoted as i, is set to 60. The system order, represented by n, is automatically determined to be equal to i after performing SVD computation. The results suggest that the stochastic subspace identification model has sufficient accuracy to be employed for monitoring the vehicle suspension system.

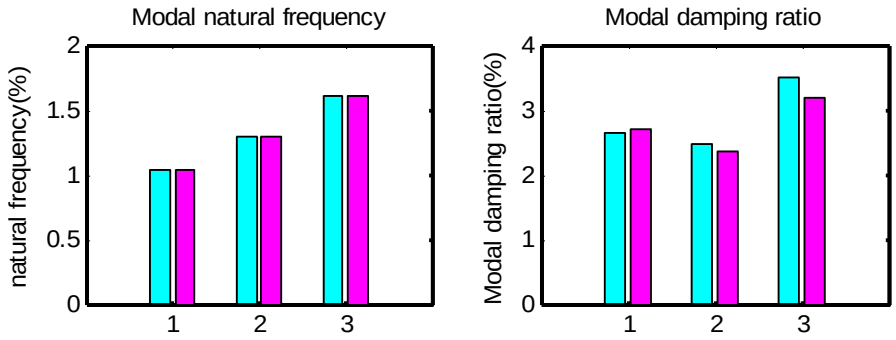

Figure 13 results of subspace identification as a comparison between theatrical values (calculated from equations) and the values obtained from the model for natural frequencies and damping ratios of the bounce, pitch and roll modes respectively.

Figure 14 displays the discrepancies in estimating the modal natural frequency and modal damping ratio for various damping coefficients in the bounce (vertical), pitch, and roll modes. From this figure, it is evident that the estimation error values for the modal natural frequency are below 1 percent for bounce and roll modes, while they exceed 3 percent for pitch modes. The estimation error for the modal damping ratio exceeds 10 percent in both the bounce and roll modes, but in the case of pitch modes, it exhibits significant variability with an approximate value of 30 percent.

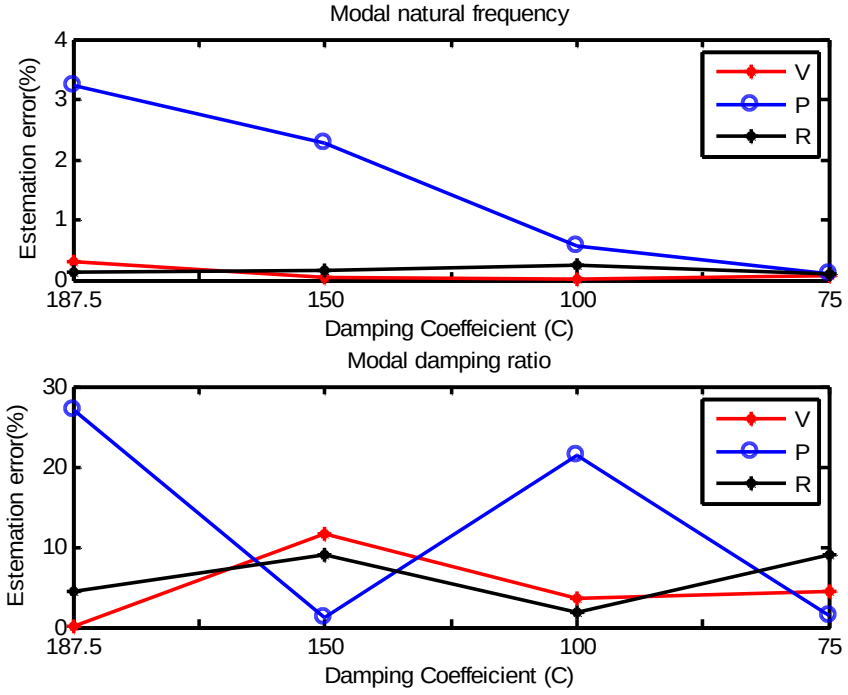

Figure 14 shows estimation errors of modal natural frequency and modal damping ratio for different damping coefficients.

Figure 15 displays the discrepancies in estimating the modal natural frequency and modal damping ratio for various spring rates in the bounce (vertical), pitch, and roll modes. This figure demonstrates

that the estimation error values for the modal natural frequency are below 1 percent for the bounce and roll modes, but the error increases to above 7 percent for the pitch modes. The estimation error values for the modal damping ratio are around 10 percent for the bounce and roll modes, whereas they exhibit significant fluctuations for the pitch modes, with values around 80 percent.

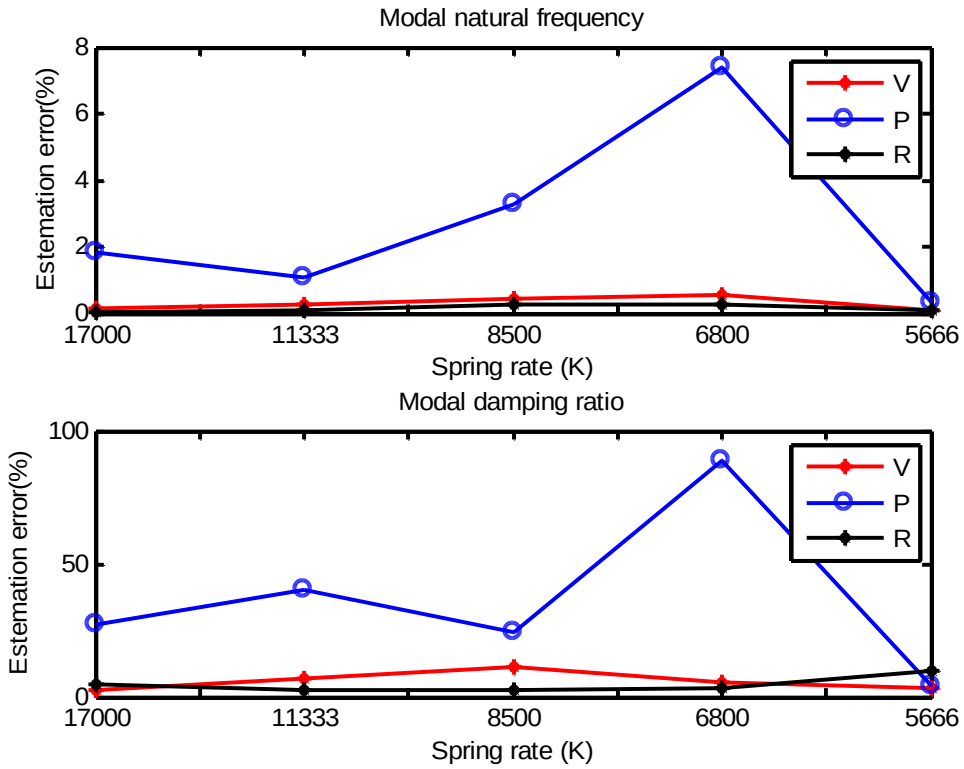

Figure 15 shows estimation errors of modal natural frequency and modal damping ratio for different spring rates.

Conclusion

The system identification technique is utilized to obtain an estimation of a set of uncertain vehicle parameters and to examine the condition monitoring of the suspension system. The formulation of system identification involves the utilization of an output error model. The system identification procedure involves generating road-tyre excitation signals that follow a white Gaussian random process. The loss function and the final prediction error function are minimized in order to determine the model structure and the system function, while accounting for different amounts of measurement noise. The results indicate that the model parameters, specifically the natural frequencies and damping ratios of the bounce, pitch, and roll modes for the whole vehicle model, can be accurately recognized with satisfactory precision. The model findings exhibited a far higher degree of proximity to the theatrical results. Furthermore, the estimation of the natural frequency demonstrates remarkable accuracy, however the assessment of damping exhibits significantly greater fluctuations compared to the frequency estimations.

References

[1] H. John, “Good Garages | Honest John.” [Online]. Available: http://good-garage-guide.honestjohn.co.uk/. [Accessed: 28-Aug-2013].

[2] B. L. Zohir, “Ride Comfort Assessment in Off Road Vehicles using passive and semi-active suspension.” [Online]. Available: http://www.academia.edu/632500/Ride_Comfort_Assessment_in_Off_Road_Vehicles_using_passive_and_semi-active_suspension. [Accessed: 23-Feb-2014].

[3] T. Weispfenning, “Fault Detection and Diagnosis of Components of the Vehicle Vertical Dynamics,” *Meccanica*, vol. 32, no. 5, pp. 459–472, Oct. 1997.

[4] A. Mitra, N. Benerjee, H. Khalane, M. Sonawane, D. Joshl, and G. Bagul, “Simulation and Analysis of Full Car Model for various Road profile on a analytically validated MATLAB/SIMULINK model,” *IOSR J. Mech. Civ. Eng. IOSR-JMCE*, pp. 22–33.

[5] Ahmad Faheem, Fairoz Alam, and V. Thomas, “The suspension dynamic analysis for a quarter car model and half car model,” Dec-2006. [Online]. Available: http://good-garage-guide.honestjohn.co.uk/mot-results/. [Accessed: 28-Aug-2013].
[6] R. Rao, T. Ram, k Rao, and P. Rao, “Analysis of passive and semi active controlled suspension systems for ride comfort in an omnibus passing over a speed bump,” Oct-2010. [Online]. Available: http://connection.ebscohost.com/c/articles/55558201/analysis-passive-semi-active-controlled-suspension-systems-ride-comfort-omnibus-passing-over-speed-bump. [Accessed: 28-Aug-2013].
[7] N. Eslaminasab, M. Biglarbegian, W. W. Melek, and M. F. Golnaraghi, “A neural network based fuzzy control approach to improve ride comfort and road handling of heavy vehicles using semi-active dampers,” *Int. J. Heavy Veh. Syst.*, vol. 14, no. 2, pp. 135–157, Jan. 2007.
[8] R. Darus and Y. M. Sam, “Modeling and control active suspension system for a full car model,” in *5th International Colloquium on Signal Processing Its Applications, 2009. CSPA 2009*, 2009, pp. 13–18.
[9] P. Metallidis, G. Verros, S. Natsiavas, and C. Papadimitriou, “Fault Detection and Optimal Sensor Location in Vehicle Suspensions,” *J. Vib. Control*, vol. 9, no. 3–4, pp. 337–359, Mar. 2003.
[10] K. Kashi, D. Nissing, D. Kesselgruber, and D. Soffker, “Diagnosis of active dynamic control systems using virtual sensors and observers,” in *2006 IEEE International Conference on Mechatronics*, 2006, pp. 113–118.
[11] A. Agharkakli, G. Sabet, and A. Barouz, “Simulation and Analysis of Passive and Active Suspension System Using Quarter Car Model for Different Road Profile,” *Int. J. Eng. Trends Technol.*-, vol. 3, no. 5, 2012.
[12] S. Ikenaga, F. L. Lewis, J. Campos, and L. Davis, “Active suspension control of ground vehicle based on a full-vehicle model,” in *American Control Conference, 2000. Proceedings of the 2000*, 2000, vol. 6, pp. 4019–4024 vol.6.
[13] F. Lu, Y. Ishikawa, H. Kitazawa, and T. Satake, “Effect of vehicle speed on shock and vibration levels in truck transport,” *Packag. Technol. Sci.*, vol. 23, no. 2, pp. 101–109, 2010.
[14] P. Holdmann and M. Holle, “Possibilities to improve the ride and handling performance of delivery trucks by modern mechatronic systems,” *JSAE Rev.*, vol. 20, no. 4, pp. 505–510, Oct. 1999.
[15] E. Alvarez-Sánchez, “A Quarter-Car Suspension System: Car Body Mass Estimator and Sliding Mode Control,” *Procedia Technol.*, vol. 7, pp. 208–214, 2013.
[16] V. S. Tudon Martinez, “Fault Tolerant Control with Additive Compensation for Faults in an Automotive Damper,” 2013.
[17] B. Breytenbach and P. S. Els, “Optimal vehicle suspension characteristics for increased structural fatigue life,” Dec. 2011.
[18] G. Dong, J. Chen, and N. Zhang, “Investigation into on-road vehicle parameter identification based on subspace methods,” *J. Sound Vib.*, vol. 333, no. 24, pp. 6760–6779, Dec. 2014.
[19] X. Yang, S. Rakheja, and I. Stiharu, “IDENTIFICATION OF LATERAL DYNAMICS AND PARAMETER ESTIMATION OF HEAVY VEHICLES,” *Mech. Syst. Signal Process.*, vol. 12, no. 5, pp. 611–628, Sep. 1998.
[20] R. R. Russo M, “Car Parameters Identification by Handling Manoeuvres,” *Veh. Syst. Dyn.*, vol. 34, no. 6, pp. 423–436, 2000.
[21] T. A. Wenzel, K. J. Burnham, M. V. Blundell, and R. A. Williams, “Dual extended Kalman filter for vehicle state and parameter estimation,” in *Vehicle system dynamics*, 2006, vol. 44, pp. 153–171.
[22] K. B. Arıkan, Y. S. Ünlüsoy, İ. Korkmaz, and A. O. Çelebi, “Identification of linear handling models for road vehicles,” *Veh. Syst. Dyn.*, vol. 46, no. 7, pp. 621–645, Jul. 2008.
[23] Y. Ming, G. Xiqiang, J.-W. Zhang, X.-Q. Guan, and M. Yuan, “Application of subspace-based method in vehicle handling dynamic model identification and properties estimation,” *Int. J. Veh. Des.*, vol. 56, no. 1, pp. 125–145, Jan. 2011.
[24] *Dynamics of Flexible Multibody Systems - Rigid Finite Element Method*. .
[25] P. Eykhoff, *System Identification: Parameter and State Estimation*. Wiley-Interscience, 1974.
[26] E. Reynders and G. D. Roeck, “Reference-based combined deterministic–stochastic subspace identification for experimental and operational modal analysis,” *Mech. Syst. Signal Process.*, vol. 22, no. 3, pp. 617–637, Apr. 2008.